Unimolecular Dissociation in Allene and Propyne: The Effect of Isomerization on the Low-Pressure Rate

J. H. Kiefer,* P. S. Mudipalli, and S. S. Sidhu

Department of Chemical Engineering, University of Illinois at Chicago, Chicago, Illinois 60680

R. D. Kern, B. S. Jursic, K. Xie, and H. Chen

Department of Chemistry, University of New Orleans, New Orleans, Louisiana 70148

Received: October 24, 1996; In Final Form: March 20, 1997[⊗]

The unimolecular dissociation of the C_3H_4 isomers allene and propyne has been examined using two complementary shock-tube techniques: laser schlieren (LS) and time-of-flight (TOF) mass spectrometry. The LS experiments cover 1800−2500 K and 70−650 Torr, in 1, 2, and 4% propyne/Kr and 1 and 2% allene/Kr, whereas the TOF results extend from 1770 and 2081 K in 3% allene or propyne in Ne. The possible channels for unimolecular dissociation in the C_3H_4 system of isomers are considered in detail, using new density functional theory calculations of the barriers for insertion of several C_3H_2 into H_2 to evaluate the possibility of H_2 elimination as a dissociation route. The dominant path clearly remains CH fission, from either isomer, as suggested in earlier work, although some small amount of H_2 elimination may be possible from allene. Rate constants for the CH fission of both allene and propyne were obtained by the usual model-assisted extrapolation of LS profiles to zero time using an extensive mechanism constructed to be consistent with both the time variation of LS gradients and the TOF product profiles. This procedure then provides rate constants effectively independent of both the near-thermoneutral isomerization of the allene/propyne and of secondary chain reactions. Derived rate constants show a strong, persistent pressure dependence, i.e., a quite unexpected deviation (falloff) from second-order behavior. These rate constants are nearer first than second order even for $T > 2000$ K. They are also anomalously large; RRKM rates using literature barriers and routine energy-transfer parameters are almost an order of magnitude too slow. The two isomers show slightly differing rates, and falloff is slightly less in allene. It is suggested that isomerization is probably slow enough for this difference to be real. The anomalously large rates and falloff are both consistent with an unusually large low-pressure-limit rate in this system. Extensive isomerization of these C_3H_4 is possible for energies well below their CH fission barriers, and this can become hindered internal rotation in the activated molecule. On the C_3H_4 surface we identify three such accessible rotors. State densities for the molecule including these rotors are calculated using a previous general classical formulation. Insertion of these state densities into the RRKM model results in rates quite close to the measured magnitudes, and showing much of the observed falloff. The increase in the low-pressure rate is as much as a factor of 8; a necessary but nonetheless remarkable effect of anharmonicity on the unimolecular rate. This again demonstrates the importance of accessible isomerization and consequent hindered internal rotation on the rate of dissociation of unsaturated species.

Introduction

In this paper we report a shock tube, laser-schlieren (LS) investigation of the dissociation of the two most stable isomers of the formula C_3H_4, allene and propyne. Of necessity, this also involves a consideration of their mutual isomerization and of the various minima and transition states which are encountered in that process. The extensive isomerization in this system opens a large number of possible dissociation channels for these molecules, and these are fully considered. As part of this consideration we present new density functional theory (DFT) calculations of the barriers for some of the more problematic routes. Finally, the paper contains an extensive chain decomposition mechanism used in an attempt at modeling the entire decomposition process initiated by this dissociation, an effort supported by new time-resolved, time-of-flightf (TOF) mass spectrometer measurements of stable species in the reflected shock regime. Although the proposed mechanism does describe the available experiments, the decomposition process is very complex, and it is probably valid only in the early stages of the reaction.

This study is motivated by both the practical importance of the C_3H_4 system and its theoretical possibilities, which arise in large part from the opportunity for interaction between isomerization and dissociation. Besides, it is now believed that the primary routes to aromatics in aliphatic flames, and thence to soot formation, is through reactions of the propargyl radical, C_3H_3, the primary dissociation/decomposition product of allene and propyne.[1−6] Despite the interest generated by this realization, there have been only a few recent studies of this decomposition.

The earliest investigation of the thermal reactions of allene and propyne is that of Levush et al.,[7] who examined both the isomerization and decomposition in an atmospheric pressure flow over 900−1150 °C. They were able to show that isomerization was faster than decomposition for these conditions but did not offer a detailed mechanism for either. Both processes were subsequently observed in both allene and propyne by Lifshitz and co-workers with the single-pulse shock tube (1040−1470 K).[8] They discussed the decomposition

[⊗] Abstract published in *Advance ACS Abstracts,* May 1, 1997.

S1089-5639(96)03314-2 CCC: $14.00

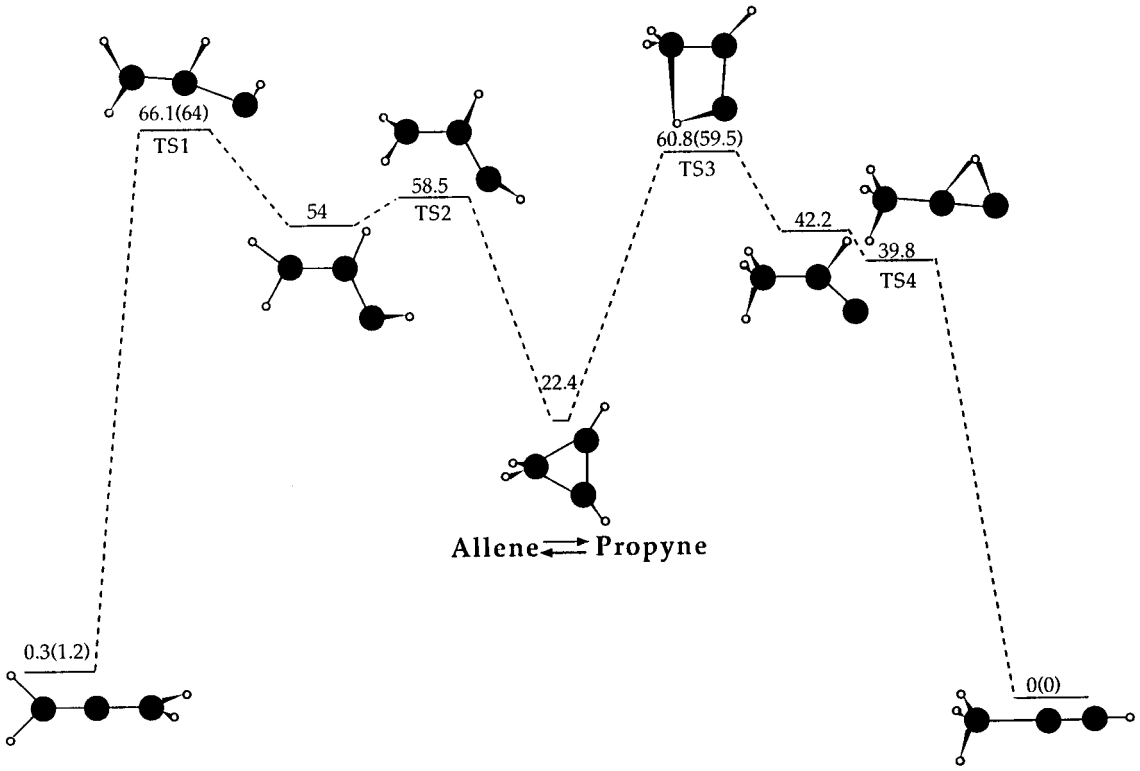

Figure 1. Minimum energy route for the mutual isomerization of allene and propyne.[13]

mechanism and suggested this was a straight chain initiated by CH fission. The subsequent shock-tube, time-of-flight (TOF) measurements of Wu and Kern, on allene, covered 1300−2000 K at lower pressures.[1] They identified many of the same species but also discovered that benzene was a major product. They offered the first detailed quantitative modeling of this pyrolysis, again assuming a straight chain initiated by CH fission. The most recent study of the decomposition (and isomerization) is that of Hidaka and co-workers,[9,10] who confirm the benzene formation and provide a quantitative mechanism similar to that of Wu and Kern, again with initiation by CH fission. Some features of these investigations are considered more fully in the Discussion.

The C_3H_4 surface is quite complex, with many minima at thermally accessible energies. This permits extensive isomerization and opens up a large number of possible dissociation routes. Much of the potential surface has been explored using ab initio methods, the aim being to identify the minimum-energy path for the mutual isomerization in allene and propyne.[11−13] The essential results of this effor are exhibited in Figure 1, where this process is seen to involve at least five such minima, which may be identified as, from right to left, propyne, methylvinylidene, cyclopropene, vinylmethylene, and allene. All of these are evidently accessible to internal energies below 65 kcal/mol. The figure shows both the theoretical energies and some slightly different numbers suggested by the available isomerization experiments. The latter come from a number of sources (see refs 9 and 14−18), all of which are discussed in ref 19, where a reversible RRKM model of the high-temperature mutual isomerization data is presented. In accord with the theoretical work[13,15,16] this model assumes passage through TS (transition state) 1 is rate-controlling. The model is in good accord with the lower temperature/higher pressure set of shock-tube experiments but disagrees with the high-temperature results of Saito et al.[16] The problem evidently lies mainly in the falloff or low-pressure-limit (LPL) behavior, where the Saito et al. data require an extremely small $\langle \Delta E \rangle_{down}$. Kiefer et al.[19] suggested that these measurements may have been distorted by parallel decomposition.

The single-pulse experiments of Lifshitz, Frenklach, and Burcat[8] clearly show the chain decomposition has a different rate and product distribution in allene than in propyne. Thus it is possible the rates and even the dissociation channels may also be different for these two. To discern any such differences, it is necessary to measure the dissociation rates before isomerization has occurred, or at least before it is complete. Lifshitz et al. were able to discern their differences in observations at their lowest temperatures where isomerization was incomplete in their heating time, but the very small amount of the slower decomposition could still be detected.

The use of LS measurements for the dissociation rate has the usual advantages. The measurements are made very early in the process, essentially in the chain induction period, thereby requiring minimal correction for chain multiplication. Such corrections often present a serious problem in the derivation of chain initiation rates from product yields. The chain should have but little effect on the LS gradients in any case. The earliest secondary processes are mainly near-thermoneutral H-atom abstractions, and the radical formed by such abstraction from C_3H_4 is the resonance-stabilized propargyl, which will not easily release another radical to continue the chain. As with toluene,[20] the C_3H_4 thus tend to act as their own chain inhibitors, and chain acceleration should be slight.

At least in principle, the LS technique should also be able to distinguish any differences in dissociation rates between allene and propyne. Here measurements are made within 1 μs of shock heating where the isomerization is very likely incomplete up to quite high temperatures. In addition, the observed dissociation density gradients will be virtually unaffected by the parallel occurrence of the near-thermoneutral isomerization ($\Delta H_{298} \sim$ 1 kcal/mol[21]), whose slight effect is overwhelmed by the much more endothermic dissociation. The LS measurements are also made at high temperatures where the reaction is fast, so any possible impurity initiation is rendered insignificant by the rapid

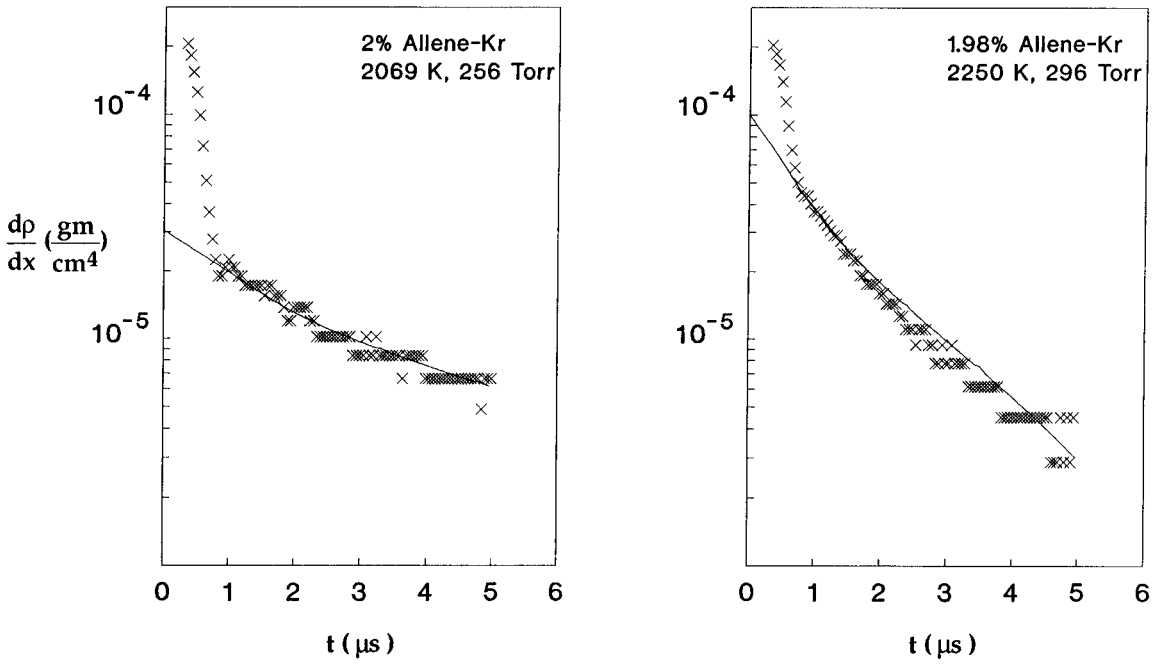

Figure 2. Example semilog plots of density gradients from experiments in allene. Here measured points are (×), and the solid lines show simulations with the mechanism of Table 2. The first set of rapidly falling points show beam-shock front interaction and should be ignored.

dissociation of the C_3H_4. All things considered, the LS technique seems a remarkably good fit to this problem.

Experimental Section

The experimental apparatus and the procedures for initial data analysis have been described in great detail for both the LS and TOF techniques[22,23] and were employed here in the usual manner. Further details were as follows.

LS Experiments. Mixtures of allene and propyne with krypton were prepared manometrically in a 50 L glass vessel with a magnetic stirrer. Allene and propyne were obtained from Solkatronic Inc., rated as 99% pure, and were used without further purification. Krypton was spectra-gases excimer grade. Some 157 LS experiments were analyzed in mixtures of 1% allene−Kr (27 experiments), 2% allene−Kr (61), 1% propyne−Kr (16), 2% propyne−Kr (37), and 4% propyne−Kr (17). Refractivities of allene and propyne were taken as the mean of the values given by Gardiner et al.[24] and assumed constant during isomerization/dissociation. Although this can only be approximately correct, the Kr carries more than 90% of the refractivity even in the 4% propyne mixture. All measurements were made in incident shock waves produced by spontaneous burst of Mylar diaphragms. Vibrational relaxation in these molecules is too fast to resolve, even at lower pressures, so initial conditions were calculated by solution of the one-dimensional conservation equations assuming chemically frozen, vibrationally relaxed ideal gases, using allene/propyne heat capacities calculated from the vibrational frequencies given by Shimanouchi.[25] The LS experiments then covered post-shock frozen conditions of 1700−2500 K and 100−650 Torr.

TOF Experiments. Four mixtures were prepared for the TOF experiments: 3% allene−Ne, 3% allene−5% H_2−Ne, 3% propyne−Ne, and 3% propyne−H_2−Ne. The two mixtures containing H_2 allowed a test of the effect of this reactant. Reagents were purchased from Matheson and from Farchain Laboratories Inc., and the C_3H_4 were double-distilled prior to mixture preparation. All peak heights seen in mass spectrometric analyses were attributable to the reagents. The experiments covered reflected-shock initial conditions of 1690−2090 K and 240−330 Torr.

Results

A. LS Experiments. Example LS density gradient profiles which typify the entire set of 157 experiments analyzed are shown in the semilog plots of Figures 2−5. With the exception of some high-pressure, low-temperature experiments (see below), these profiles show a consistent near-linear (exponential gradient) to slightly concave shape as would be expected of a very weak chain reaction. A strong chain will produce an initially rising gradient leading to a convex profile, even a maximum,[26,27] whereas a dissociation which does not initiate a following chain, i.e., a molecular reaction,[28−30] creates a strongly concave shape; the single endothermic reaction slows as the temperature drops. The behavior seen here is actually much like that in toluene,[20] and it is very likely the mechanistic situation is also similar. Initiation is bond fission, but the resulting radical chain is inhibited by the parent molecule. In toluene it is the stability of the benzyl product which inhibits chain propagation; here it is the fault of the propargyl radical. They may not be decisive in themselves, but these simple observations are certainly consistent with the earlier notion that the initiation dissociation in the C_3H_4 is C−H bond fission. The solid lines on these figures show the results of simulations with the mechanism presented in the Analysis.

B. TOF Experiments. A representative set of TOF product profiles is shown in Figures 6 and 7. These are similar to a set previously published,[1] again showing C_2H_2, CH_4, C_4H_2, and C_6H_6 as major products. The lines again show the results of simulation with the mechanism detailed below.

Analysis

Although the above results seem to indicate initiation is indeed through C−H fission, there are quite a number of possible dissociation channels, and some of these may well mimic such behavior. Thus it is appropriate to attempt a full treatment of this issue. This discussion necessarily begins with a consideration of the product thermochemistry, and the heats of formation selected here for various possible dissociation products are listed in Table 1. The origins of these either are given in the table or are discussed below. Other properties,

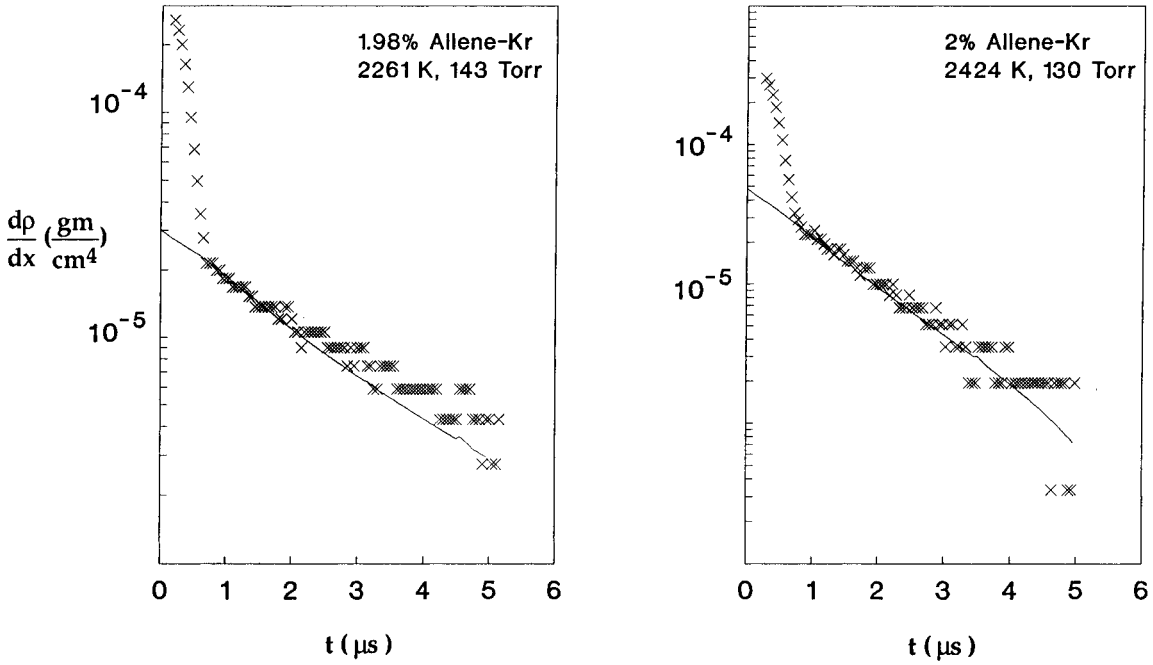

Figure 3. Further examples of gradients in allene (see Figure 2).

entropies and heat capacities, were either taken from standard sources[32,36] or calculated from molecular properties given in the references listed in Table 1. Given this thermochemistry, the following seem to be all the channels which might possibly be involved at LS and TOF temperatures. Starting from propyne (P−C_3H_4), these are

1. C-H fission:

   a. Direct: $P-C_3H_4 \rightarrow C_3H_3 + H$ $\quad \Delta H^\circ_0 = 92.5 \pm$ kcal/mol

   b. Via cyclopropene:

   $$P-C_3H_4 \rightarrow c\text{-}C_3H_4 \rightarrow c\text{-}C_3H_3 + H \qquad \sim 112^{38}$$

2. C−C fission:

   $$P-C_3H_4 \rightarrow CH_3 + C_2H \qquad 124 \pm 1$$

3. $^1CH_2$ elimination:

   $$P-C_3H_4 \rightarrow {}^1CH_2 + C_2H_2 \qquad 111 \pm 1$$

4. H_2 elimination:

   a. through allene:

   $$P-C_3H_4 \rightarrow CH_2{=}C{=}CH_2 \rightarrow CH_2{=}C{=}C{:} + H_2 \qquad 85 \pm 4$$

   b. through cyclopropenylidene:

   P-C_3H_4 → 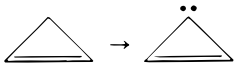 + H_2 $\qquad$ 70±4

The H_2 eliminations are most favorable thermochemically but are complex eliminations which are expected to have substantial reverse barriers, i.e., to have forward barriers larger than the endothermicity. To obtain a good estimate of the last two barriers, we have performed DFT calculations of the transition-state energies, calculations whose details are reported in the Appendix. The result is a rather small reverse barrier of 3.6 kcal/mol for the channel involving H_2 elimination from allene, and a large barrier of 32.3 kcal/mol for elimination from cyclopropene, a figure in close agreement with a much earlier study of this reaction.[40] We thus conclude that CH fission, with no reverse barrier, or H_2 elimination (from allene), are the only feasible dissociation routes from C_3H_4.

Our best estimate of the barrier for H_2 elimination from allene is only 88.6 kcal/mol, 3.9 kcal/mol below the barrier for CH fission. Unfortunately, the combined uncertainty in these figures is larger than their difference, and it is impossible to make an accurate estimate of their relative contribution to dissociation. Nonetheless, the difference in barrier must be small, and the entropy of activation should largely determine the dominant channel for this pyrolysis. As long as the reaction remains in the falloff region, and it does (see below), then bond fission should certainly dominate. The available literature evidence[1,8−10] also supports a dominance by CH fission, which may reflect the much larger HPL *A*-factor expected from the very loose transition state for such fission.

To extract accurate dissociation rate constants from LS gradient profiles usually requires a secondary mechanism, so that they can be extrapolated through the first 0.5−1 μs to the time origin, where the state of the gas is unambiguous (vibrationally relaxed, but chemically frozen) and only the initial dissociation occurs. Here, of course, there is also the parallel, and possibly faster, isomerization. But this is near thermoneutral and contributes little to the gradient. In the present analysis, it is assumed that isomerization is slow enough so that the initial gradient is entirely from dissociation of a single isomer (see below for further consideration of this issue). Thus the analysis provides a separate rate for each of the two parent C_3H_4 isomers.

The mechanism can also be used to define both the secondary reaction gradients and the state of the gas throughout the observation, so that all the measured points are then used for the dissociation rate. Either method normally requires iteration; a complete description of the procedure has been given in another context.[30] In the present instance the near linearity of the profiles allows a good first estimate of the initial gradient by straight-line extrapolation, and only a slight increase in the rate constants actually results from the detailed modeling described in the following section.

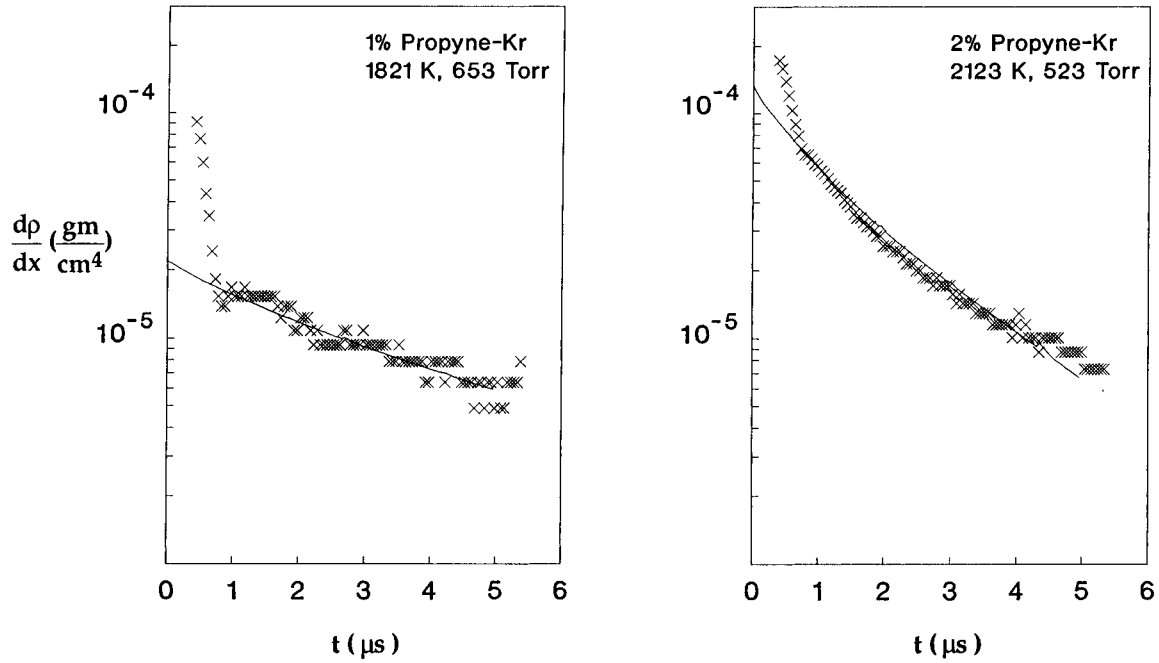

Figure 4. Examples of density gradients measured in propyne. Refer to Figure 2 for details.

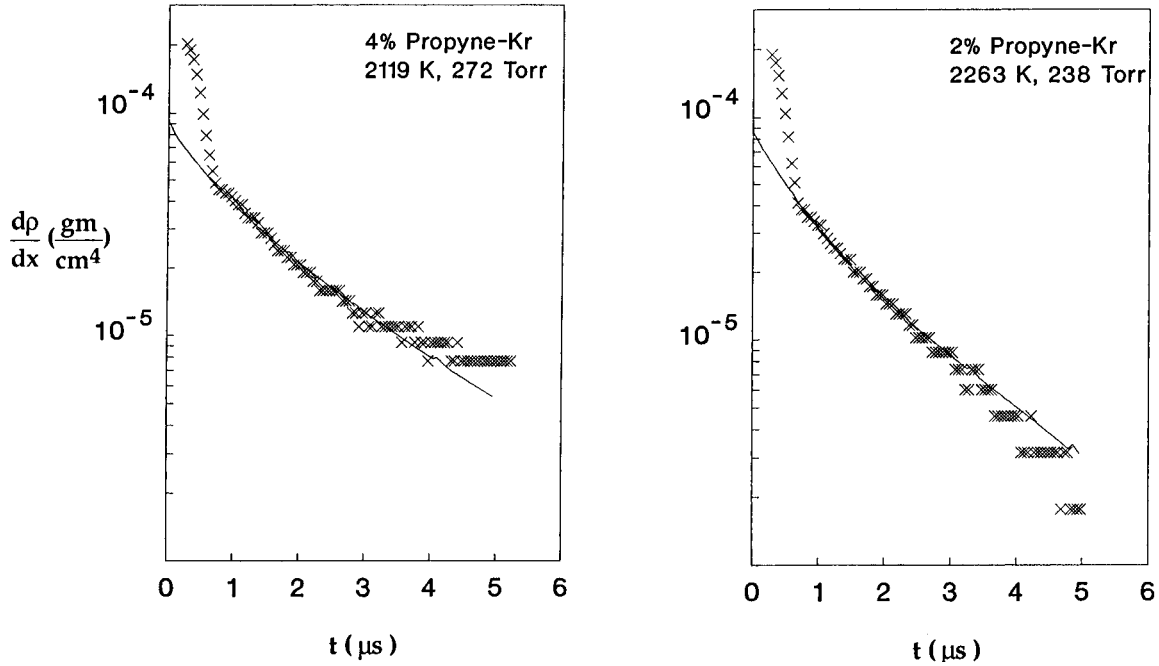

Figure 5. Further examples of gradients in propyne. Again see Figure 2.

The C−H fission rate constants derived as described here are presented in the second-order Arrhenius plots of Figures 8 and 9. The rate constants are plotted second-order to emphasize their pressure dependence when presented this way, i.e., their strong deviation from the LPL. In propyne, these rate constants are actually nearer first than second order. The implications of this surprising behavior are considered in the Discussion.

It is always difficult to set quantitative error limits on dissociation rates derived from LS measurements because the extrapolation, whose accuracy depends in part on the validity of the pyrolysis mechanism, may well be the main cause of any systematic error. This cannot be very large here both because the semilog plots are close to linear, so that extrapolation is almost independent of the modeling, and because the mechanism, whatever its faults, is also an excellent fit of the entire gradient profile quite generally. The greatest source of random error in the LS experiments has already[30] been identified as the $\pm(1-2) \times 10^{-6}$ g/cm^4 accuracy of gradient determination. Here this contributes in the vicinity of a $\pm 10\%$ uncertainty in rate constant in the center of the temperature range but is somewhat larger at lower temperatures and smaller at the high end. All things considered, the scatter seen in Figures 8 and 9 probably remains the best estimate of the uncertainty in these rate constants.

These rate constants also accurately describe the decay of the parent C_3H_4 and major product (C_2H_2) formation in the TOF experiments, as exemplified in the simulations of Figures 6 and 7. Here there are minor discrepancies in the lesser products, which is always a difficulty in a pyrolysis which ultimately generates copious soot. For example, the overprediction of C_4H_2 may well indicate loss of this species to solid formation. The

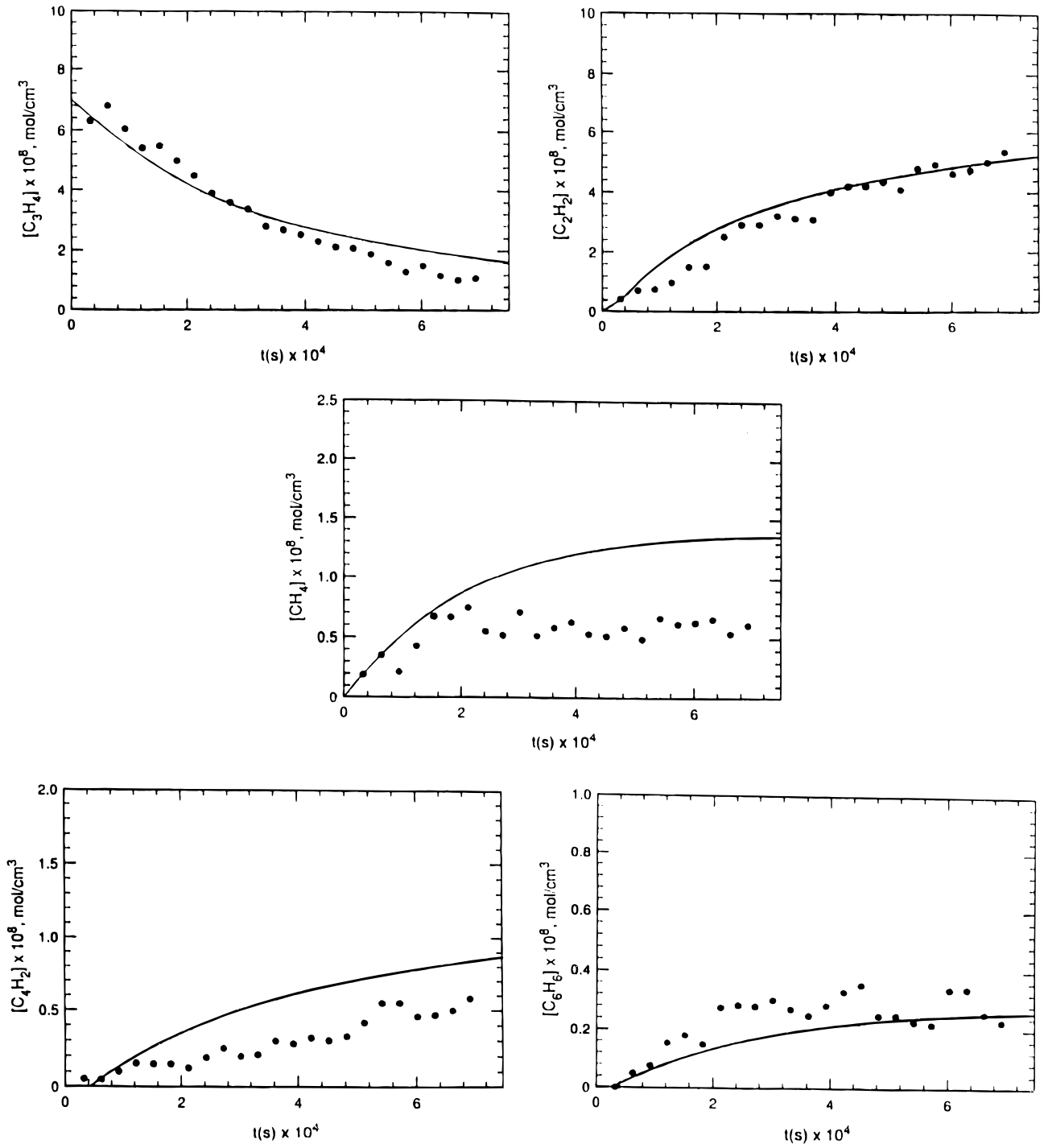

Figure 6. TOF parent and product profiles from an experiment in 3% allene at 2081 K and 0.44 atm. The solid circles are the measured concentrations, and the lines show simulations using the mechanism of Table 2.

important point as concerns the dissociation rate is again the very satisfactory description of parent decay and total product generation. Here there is one significant change in the interpretation. The simulation C_3H_4 concentrations now have all the C_3H_3 added in, because we suspect it is not possible to separate these masses in the experiments. There are significant concentrations of C_3H_3 formed in this reaction, and they must be included somewhere. Their inclusion in the C_3H_4 signal extends the tail of this profile resulting in a much better accord with the data. For the two examples illustrated in Figures 6 and 7, the C_3H_3 is negligible throughout the 1770 K experiment but reaches 30% of the total C_3 at 70% completion in the 2087 K example of Figure 7.

Secondary Reaction Mechanism. The full mechanism used in the modeling of the LS and TOF data is given in Table 2. This should be regarded as a "short version", set up primarily to deal with the pyrolysis at the early times, 0−2 μs, needed for the extrapolation of LS gradients through the initial spike caused by shock-front passage. Although this mechanism provides a good fit to most of the LS profiles over their entire length (Figures 2−5), and does quite well with the much longer duration TOF data (see Figures 6 and 7), this is an extremely complex decomposition when fully underway, and the mechanism cannot be much more than schematic. Nonetheless, it appears to be more than adequate for its principal short-time purpose. The mechanism is largely based on previous

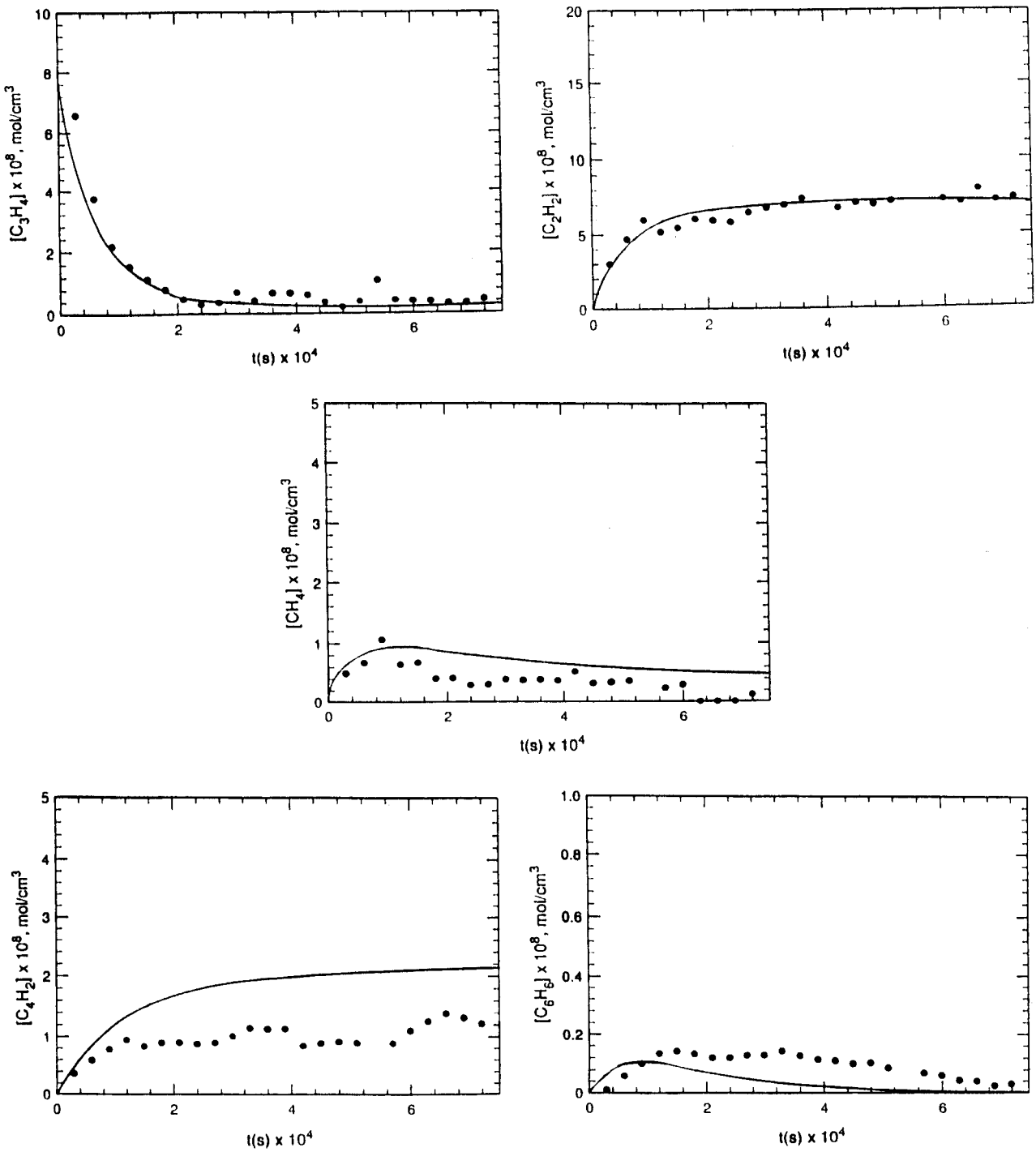

Figure 7. TOF parent and product profiles for 3% propyne at 1770 K and 0.34 atm. See Figure 6.

schemes.[1,9,10] Some chosen variations and particularly important segments are discussed here.

1. Isomerization. A fairly complete consideration of the allene/propyne isomerization was previously published,[19] and this was discussed in the Introduction. The choice of rate expression finally employed here is a compromise between the high-temperature measurements of Kakumoto et al.[16] and our own RRKM modeling of the lower-temperature data. If the largest proposed $\Delta H°_0$, 1.4 kcal/mol,[21] is used for propyne → allene, together with the fastest (RRKM) rate constants, a small initial gradient of very short duration appears in the model calculations. This is not observed and is thought to be artificial. Reduction of either the heat of reaction or the rate will eliminate this phenomenon, and we have chosen to reduce the rate. The exact heat of reaction is also uncertain, with literature values ranging from 0.3 to 1.4 kcal/mol.[13,17,21]

Unfortunately, it is not presently possible to set a fully convincing LPL isomerization rate which would be applicable for high temperatures and low pressures; the only data[16] suggest a rate so low that unreasonable parameters are required for an RRKM fit.[19] In this paper we shall assume that isomerization is slow enough that the LS experiments can distinguish independent dissociation rates in the two isomers. Our isomerization rates are thus reduced from those used before[19] to fit the lower temperature measurements but are still faster than those proposed by Kakumoto et al. This seems a reasonable if somewhat unsatisfying compromise. However, as long as isomerization is anywhere near this slow, it does not matter

TABLE 1: Heats of Formation and $H°_{298}-H_0°$

species	$\Delta_f H°_{298}$ (kcal/mol) [source]	$H°_{298} - H_0°$ (kcal/mol)
A-C_3H_4	45.4 [21]	3.0131[f] [*a*]
P-C_3H_4	44.2 [11]	3.1442[f] [*a*]
c-C_3H_4	66.2 [21]	
C_3H_3	85.9 [see text]	2.9862[f] [*b*]
H	52.1 [32]	1.4810 [32]
C_2H	135.5 [32]	2.4987 [32]
CH_3	35.6 [32]	2.4870 [32]
C_2H_2	54.5 [32]	2.3939 [32]
CH_2 (singlet)	99.8 [32]	2.3747 [32]
C_3H_2 (propadienylidene)	127.5 [34,35]	2.9831[f] [*c*]
C_3H_2 (cyclopropenylidene)	114 [34]	2.5472[f] [*d*]
C_3H_2 (triplet propargylene)	123.6 [34, 35]	3.4778[f] [*e*]

[a] References 25 and 36. [b] Reference 37. [c] Reference 38. [d] Reference 39. [e] Reference 35. [f] Calculated using vibrational frequencies and moments of inertia from literature values.

what rates are actually used in the modeling. Note that the mechanism also contains a catalytic isomerization path through addition and then loss of H atoms (reaction 2) with an estimated rate.

2. Formation of Benzene and Phenyl Radical. Perhaps the most important observation coming out of the earlier studies of C_3H_4 pyrolysis is the TOF mass spectrometric identification of benzene as a major product.[1] This discovery has now motivated numerous investigations of the origin of the benzene,[2−6] including a detailed ab initio investigation of the paths available beginning with C_3H_3 dimerization, which are reproduced in Figures 10 and 11. It has even been suggested that this is the principal route to aromatics in aliphatic flames.[5] Westmoreland[41] has suggested that other C_6H_6 isomers might actually dominate the 78 amu mass peak, but our modeling shows that this is most unlikely at the present high temperatures. The three high-entropy "linear" dimers (heats of formation are by group additivity)

	$\Delta_f H°_{298}$ (kcal/mol)
$CH_2{=}C{=}CH{-}CH{=}C{=}CH_2$ (tail-to-tail propargyl)	92
$CH{\equiv}C{-}CH_2{-}CH_2{-}C{\equiv}CH$ (head-to-head)	101
$CH{\equiv}C{-}CH_2{-}CH{=}C{=}CH_2$ (head-to-tail)	95

are found to be unstable with respect to redissociation into C_3H_3 radicals, and the most energetically stable isomer, fulvene, is nowhere near stable enough. Thus the identification of this mass as benzene seems quite unambiguous.

There are several possible routes to benzene in the pyrolysis of C_3H_4 isomers. The path through dimerization of C_3H_3 is solidly established, both experimentally[2] and theoretically,[6] but there are other possibilities that should be recognized. One proposed in the original TOF paper[1] is the addition/elimination

$$C_3H_4 + C_3H_3 \rightarrow C_6H_6 + H$$

Here the C_6H_6 would initially be one of the above linear isomers, which again isomerizes to benzene as in Figures 10 and 11. This process seems quite likely but is not included in the model of Table 2 because it is still conjectural. Studies of the pyrolysis of propagyl halides[42,43] would, however, seem to suggest that this could be an important route.

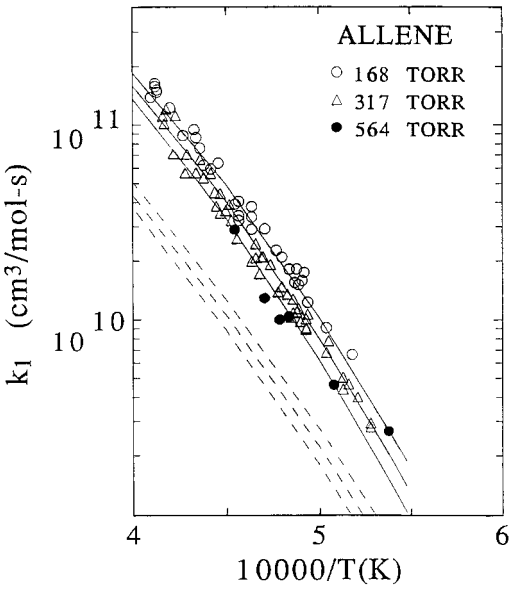

Figure 8. Arrhenius plot of second-order rate constants for the C−H fission of allene. The measurements are grouped by pressures as (○) 70−200 Torr, (△) 201−500 Torr, and (●) 501−700 Torr. Composition was found to have no discernible effect and is not specified. The dashed lines show the results of the "standard" RRKM model calculation specified in Table 6, and the solid lines that of the hindered-rotor model of Table 7. Both sets show the results for the mean pressure cited in the figure.

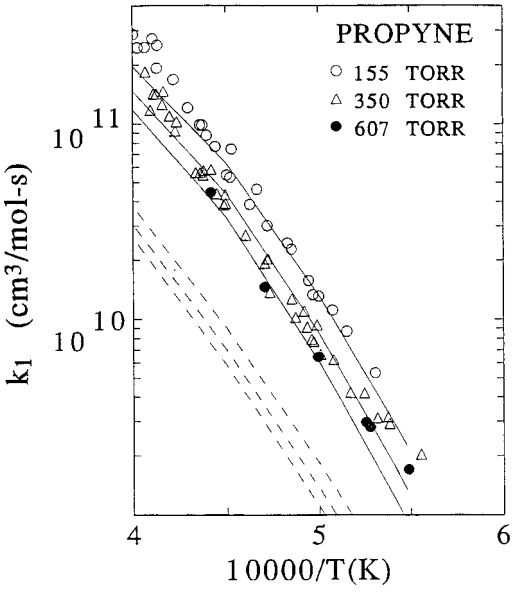

Figure 9. Arrhenius plot of second-order rate constants for the C−H fission of propyne. The data are grouped into the same pressure ranges, and the lines also have the same assignments as in Figure 8, for the mean pressures on the figure. Again the composition was not found to have a discernible effect.

One example possibility for benzene formation, for which there is some evidence,[44,45] begins with allene dimerization and might proceed as follows:

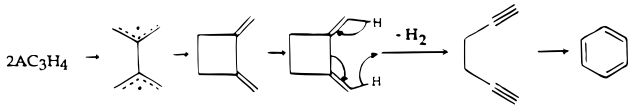

This seems a rather good low-temperature path, but is unlikely to contribute much under present conditions. Evidently this can also generate C_2H_4 and C_4H_4 through[17]

TABLE 2: Reaction Mechanism

reaction[a]	log A^b	n	E	$\Delta H°_{298}{}^c$	source
(1) A-C_3H_4 + M → P-C_3H_4 + M		see text		−1.10	est
(2) A-C_3H_4 + H → P-C_3H_4 + H	13.40	0.00	0.00	−1.10	est
(3) A-C_3H_4 + M → C_3H_3 + H + M		see text		92.65	pw
(4) P-C_3H_4 + M → C_3H_3 + H + M		see text		93.75	pw
(5) P-C_3H_4 + H → C_2H_2 + CH_3	5.12	2.50	1.00	−6.36	[10]
(6) A-C_3H_4 + H → C_3H_3 + H_2	6.70	2.00	6.00	−11.55	est
(7) P-C_3H_4 + H → C_3H_3 + H_2	14.30	0.00	15.00	−10.45	est
(8) A-C_3H_4 + CH_3 → C_3H_3 + CH_4	−3.18	5.00	8.30	−12.95	[65]
(9) P-C_3H_4 + CH_3 → C_3H_3 + CH_4	−3.66	5.00	8.30	−11.85	[65]
(10) CH_4 + M → CH_3 + H + M	17.33	0.00	88.40	105.60	[66]
(11) CH_4 + H → CH_3 + H_2	4.34	3.00	8.70	1.40	[66]
(12) C_4H_3 + M → C_4H_2 + H + M	16.30	0.00	45.00	49.10	est
(13) C_3H_3 + M → C_3H_2 + H + M		see text		89.65	est
(14) $2C_3H_3$ → C_6H_6		see text		−152.10	est
(15) $2C_3H_3$ → C_6H_5 + H		see text		−38.00	est
(16) C_6H_6 → C_6H_5 + H	15.70	0.00	107.90	114.10	[67]
(17) C_6H_6 + H → C_6H_5 + H_2	14.40	0.00	16.00	9.90	[27]
(18) C_6H_5 + M → C_2H_2 + C_4H_3 + M	15.60	0.00	37.00	86.52	[27]
(19) $2CH_3$ → C_2H_5 + H	13.10	0.00	11.30	7.36	[68]
(20) C_2H_4 + H + M → C_2H_5 + M	17.10	0.00	0.00	−38.14	[65]
(21) $2C_2H_2$ → C_4H_3 + H	14.20	0.00	56.00	57.06	[33]
(22) C_4H_3 + H → C_4H_2 + H_2	13.30	0.00	0.00	−55.10	[33]
(23) C_3H_3 + H → C_3H_2 + H_2	13.00	0.00	0.00	−14.55	est
(24) C_3H_3 + CH_3 → $2C_2H_2$ + 2H	11.80	0.00	0.00	91.57	est
(25) $^1CH_2$ + C_2H_2 → C_3H_3 + H	14.60	0.00	0.00	−16.15	est
(26) $^1CH_2$ + H → $^3CH_2$ + H	14.00	0.00	0.00	−7.43	est
(27) $2C_3H_2$ → C_2H_2 + C_4H_2	12.30	0.00	0.00	−81.68	est
(28) $2(^3CH_2)$ → C_2H_2 + H_2	13.00	0.00	0.00	−130.18	est
(29) C_3H_2 + $^3CH_2$ → $2C_2H_2$	12.30	0.00	0.00	−106.91	est

[a] The reverse of each reaction is included through detailed balance. [b] Rate expressions are of the form: $\log k$ (cm^3/mol s) = $\log A + n \log T - E/2.303RT$ (kcal/mol). [c] $\Delta H°_{298}$ in kcal/mol.

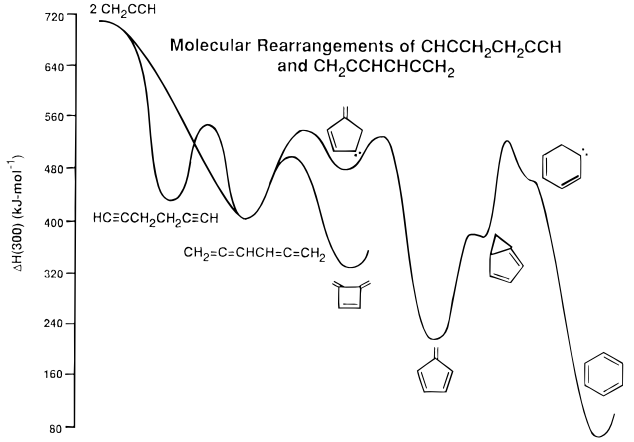

Figure 10. BAC-MP4 reaction pathway diagram[6] for the molecular rearrangement of C_6H_6 species involving 1,5-hexadiyne and 1,2,4,5-hexatriene.

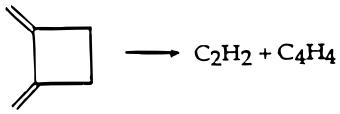

The reaction $2C_3H_3 \rightarrow C_6H_6$ (14) is 152 kcal/mol exothermic, and it is probable only a small fraction of the benzene thus formed can be stabilized at high temperatures. Most of the reaction probably proceeds to C_6H_5 + H (15), which is still 38 kcal/mol exothermic. This is an important reaction at high temperatures; in the present model phenyl decomposition is the source of most of the dominant products, acetylene and diacetylene (Figures 6 and 7). The treatment of this chemical activation problem is extremely difficult because of the very complex, many stage path to benzene. The main problem with this process lies in setting the fractions of the numerous intermediates which move forward toward benzene in the full schemes shown here in Figures 10 and 11. In this schematic mechanism we have reduced the transformation to two steps, an initial combination followed by direct isomerization to benzene. The TS properties for benzene CH fission and its stabilization efficiency are both available[27] and are listed in the RRKM model detailed in Table 3. These were then used in a further RRKM estimation of the stabilization (Table 4), thus setting the branching between reactions 14 and 15.

Aromatic formation may well be the most important issue in this pyrolysis, but it is a difficult problem and is at most peripheral to the issue at hand, the extraction of an accurate dissociation rate, so further discussion shall be left to another place.

3. Propargyl Dissociation. At the high temperatures of the present LS and TOF experiments, further reaction of otherwise stable product species is possible. An important instance introduced here is either dissociation or H-atom abstraction from the propargyl radical, the dominant radical formed in this chain decomposition. It is evidently one of the pair hydrogens which is most easily removed forming triplet propargylene ($\Delta H°_{298}$ values from Table 1)

$$CH_2{=}C{=}CH + M \rightarrow HC{=}C{=}CH + H + M \quad (89.8) \quad (13)$$

or through abstraction

$$C_3H_3 + H \rightarrow C_3H_2 + H_2 \quad (-14.4) \quad (23)$$

The properties of the propargylene were taken from the ab initio calculations of refs 34 and 35. Although the cyclopropenylidene is the most stable C_3H_2 energetically, the triplet propargylene is by far the dominant isomer at equilibrium, as shown in Figure 12. The rates used for these were taken from those of similar reactions for the abstraction, and standard-model RRKM

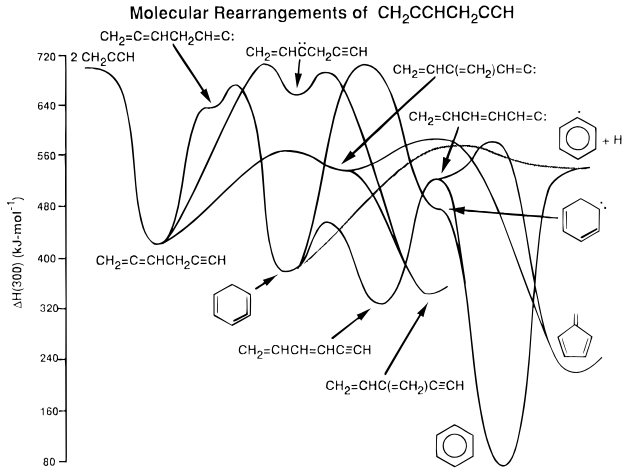

Figure 11. BAC-MP4 reaction diagram[6] for the molecular rearrangement of C_6H_6 species involving 1,2-hexadien-5-yne.

TABLE 3: RRKM Parameters for $C_6H_6 \rightarrow 2C_3H_3$

frequencies (cm^{-1})	
benzene[a]	3062, 992, 1326, 673, 3068, 1010, 995, 703, 1310, 1150, 849, 849, 3063, 3063, 1486, 1486, 1038, 1038, 3047, 3047, 1596, 1596, 1178, 1178, 606, 606, 975, 975, 410, 410
TS1[b]	3310, 3310, 3105, 3105, 3010, 3010, 2107.8, 2107.8, 1445.4, 1445.4, 1044, 1044, 964.8, 964.8, 787.5, 787.5, 766.85, 766.85, 548, 548, 483, 483, 406, 406
active moments of inertia (amu Å^2)	
benzene[a]	TS[b]
175.76	1.7, 53.76, 55.46 (all degeneracy of two)
I^+/I	$2.15(E_0/kT)^{1/3}$
$E_0 = \Delta H°_0$ (kcal/mol):	149.52
$\langle\Delta E\rangle_{all}$ (cm^{-1})	-70
restriction parameter	$\eta = 1.0 - 2.5/T$
reaction path degeneracy	$L^‡ = 6$
σ (Å)	4.776
ϵ/k (K)	638.31

[a] Reference 36. [b] Reference 37.

calculations (see Table 5) for the dissociation, about a factor 3 slower than the parent reaction.

4. Other Reactions. It is assumed that reaction with CH_3 is primarily the addition/dissociation of (24), which is the overall result of a multistep process consisting of recombination to 1,2-butadiene, followed by chemically activated CH fission, further CH fission of the resulting C_4H_5, and finally C_4H_4 dissociation into acetylenes.[46]

Some other overall recombination reactions included in the model are presumed to follow the more detailed paths:

$$2HC{=}C{=}CH \rightarrow HC{=}C{-}CH{=}CH{-}C{=}CH \rightarrow C_2H_2 + C_4H_2 \quad (27)$$

The last step requires two H-atom migrations.

$$^3CH_2 + {}^3CH_2 \rightarrow H_2C{=}CH_2 \rightarrow H_2C{=}C{:} + H_2 \rightarrow C_2H_2 + H_2 \quad (28)$$

For reaction 29 the dissociation is chemically activated:

$$^3CH_2 + HC{=}C{=}CH \rightarrow H_2C{=}C{=}C{=}CH_2 \rightarrow 2C_2H_2 \quad (29)$$

TABLE 4: RRKM Parameters for $C_6H_6 \rightarrow C_6H_5 + H$

frequencies (cm^{-1})	
benzene[a]	3062, 992, 1326, 673, 3068, 1010, 995, 703, 1310, 1150, 849, 849, 3063, 3063, 1486, 1486, 1038, 1038, 3047, 3047, 1596, 1596, 1178, 1178, 606, 606, 975, 975, 410, 410
TS1[a]	3062, 992, 1326, 673, 3068, 1010, 995, 703, 1310, 1150, 849, 849, 3063, 1486, 1486, 1038, 3047, 3047, 1596, 1596, 1178, 1178, 606, 606, 975, 410, 410
active moments of inertia (amu Å^2)	
benzene[a]	TS[a]
175.76	83.05, 89.38, 172.43
I^+/I	$2.15(E_0/kT)^{1/3}$
E_0 (kcal/mol)	112[b]
$\langle\Delta E\rangle_{all}$ (cm^{-1})	-70
restriction parameter	$\eta = 1 - 10/T$
reaction path degeneracy	$L^‡ = 6$
σ (Å)	4.776
ϵ/k (K)	638.31

[a] Reference 36. [b] Reference 37.

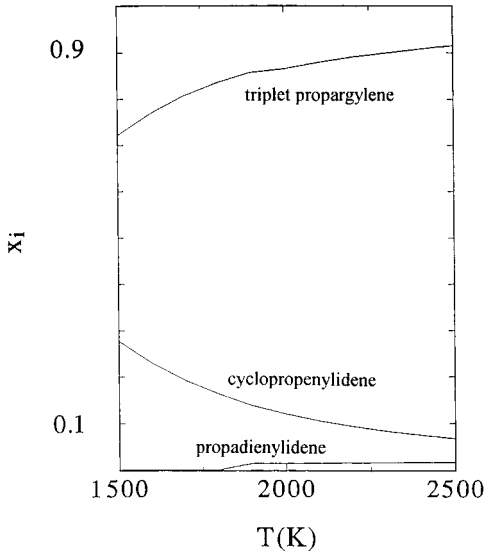

Figure 12. Equilibrium fractions of principal C_3H_2 isomers as indicated.

and may involve a prior isomerization of the cumulene to vinylacetylene.

This is a very complex decomposition, and the inadequacy of the present mechanism must be emphasized. There are numerous, and obvious, additional reactions of the above radicals not recognized. For example, reaction of CH_2 with the parent or with other radicals as well as products such as benzene. This mechanism merely performs its primary function, the provision of a satisfactory description of the LS and TOF profiles which can be used in a reliable extrapolation of the LS gradients to the time origin.

Discussion

Given a bond energy for CH fission of 92.5 kcal/mol and the known frequencies of both of the C_3H_4 and the C_3H_3 radical, the only additional properties needed for a restricted-rotor Gorin model RRKM calculation of the unimolecular rate are the restriction parameter, η,[47,48] and an average collisional energy transfer; for example, $\langle\Delta E\rangle_{all}$.[49,50] These last features are not

TABLE 5: RRKM Parameters for $C_3H_3 \rightarrow C_3H_2 + H$

frequencies (cm^{-1})	
propargyl[a]	3310, 3105, 3010, 2107.8, 1445.4, 1044, 964.8, 787.5, 766.85, 548, 483, 406
TS1[b]	3156, 3153, 1480, 1081, 510, 380, 348, 338, 278
active moments of inertia (amu Å^2)	
propargyl[a]	TS[b]
55.46	0.59, 49.26, 49.85
I^+/I	$2.15(E_0/kT)^{1/3}$
$E_0 = \Delta H°_0$ (kcal/mol)	87.71
$\langle\Delta E\rangle_{down}$ (cm^{-1})	500
restriction parameter	$\eta = 1.0-2/T$
reaction path degeneracy	$L^{\ddagger} = 2$
σ (Å)	4.742
ϵ/k (K)	261

[a] Reference 37. [b] Reference 35.

TABLE 6: Standard RRKM Model for C−H Fission in Allene/Propyne

allene[a]	3015, 1443, 1073, 865, 3007, 1957, 1398, 3086, 3086, 999, 999, 841, 841, 355, 355	
propyne[a]	3334, 931, 2918, 2142, 1382, 3008, 3008, 1452, 1452, 1053, 1053, 633, 633, 328, 328	
TS (Gorin)[b]	3310, 3105, 3010, 2107.8, 1445.4, 1044, 964.8, 787.5, 766.85, 548.0, 483.0, 406	
Active Moments of Inertia (amu-Å^2):		
allene[c]	propyne[c]	TS[b]
3.34	3.18	1.7, 53.7, 55.5
I^+/I	$2.15(E_0/kT)^{1/3}$	
E_0 (kcal/mol):	92.5[d] (from propyne)	91.3[e] (from allene)
$\langle-\Delta E\rangle_{all}$ (cm^{-1}):	−60 for each	
restriction parameter: $\eta = 1.0 - 2/T$		

[a] Reference 25. [b] Reference 37. [c] Reference 36. [d] Reference 31. [e] $\Delta H°_0(A \rightarrow P) = -1.2$ kcal/mol.

available, so we begin by assuming values typical of hydrocarbon−rare gas mixtures.[51,52] The parameters of such a typical or "standard" RRKM model is given in Table 6 for both allene and propyne, where the reader should particularly note the values chosen for η and $\langle\Delta E\rangle_{all}$. The molecular frequencies in Table 6 are from Shimanouchi,[25] and the Gorin TS frequencies are those of propargyl radical.[37] This model is thus "standard" with only one other change. Now the "reversibility" of the earlier isomerization model has been included; activated molecules can be deactivated to both allene and propyne. This lowers the total rate but also increases the falloff from the LPL. Of course it is also possible to deactivate to the other minima, but these are unstable and should also revert to either allene or propyne. The resulting expression for the unimolecular rate from propyne is

$$k^{P}_{uni} = L_P{}^{\ddagger} F^{WC}_P \exp\left(-\frac{E^P_0}{kT}\right) \int_0^{\infty} \frac{\frac{G^+(E)}{hQ^P}\exp\left(-\frac{E}{kT}\right) dE}{1 + \left(L_P{}^{\ddagger}\frac{G^+(E)}{h\rho_P(E+E^P_0)}\left(\frac{1}{\beta^P_c Z^P_{L-J}[M]F_P}\right)\right) + \frac{\beta^A_c}{\beta^P_c}}$$

The equivalent expression for allene is obtained on switching all A's and P's. The $\beta_c{}^A/\beta_c{}^P$ is from deactivation to both allene and propyne, assuming the collision frequencies nearly cancel. In this expression the Q is the total molecular partition function, $G^+(E)$ is the TS state count including rotations, F is a collection of Troe factors,[49,50] the F^{WC} is a broadening correction, and the $L^{\ddagger}$ are reaction-path degeneracies (symmetry numbers). The weak-collision parameters, β_c and the F^{WC}, were calculated from the formulas of ref 59. It is recognized that these may not be appropriate for this situation (and that considered below), but there does not appear to be any superior alternative.

The results of RRKM calculation of rate constants for both isomers under LS conditions using the models of Table 6 are shown together with the experimental data in Figures 8 and 9. Obviously the calculated second-order rates are uniformly much too slow and do not show enough pressure dependence, most notably in propyne. These two difficulties are both consistent with a too small LPL rate in the calculations. In fact, direct variation of the HPL rates by the simple expedient of changing the restriction parameter can effect little improvement in the situation. Raising this increases the falloff as desired but lowers the magnitude, whereas a decrease reduces the falloff, the deviation from the LPL, while producing very little increase in rate. The problem is clearly with the LPL rate, and no acceptable modification of the HPL parameters can resolve it.

A larger LPL rate is easily obtained from the RRKM calculations by simply increasing the average energy transfer, the other "free" parameter in the model. However, the required increase is huge, up to $\langle\Delta E\rangle_{down} \sim 1700$ cm^{-1} at 2000 K ($\langle\Delta E\rangle_{all} \sim -700$ cm^{-1}), a value far larger than anything previously encountered in hydrocarbon−rare gas systems. Of course, the magnitude problem can also be ameliorated by using a smaller barrier/CH bond energy. But this again requires a very large change, far outside the error limits of the ab initio calculations.[31] Undoubtedly some combination of parameters can be made to get closer, but adequate changes are uncomfortably large, and it seems best to look elsewhere for a solution.

It now appears that this may be a rather striking example of the anharmonic enhancement in state density which can occur in molecules where there is extensive isomerization accessible to energies well below the dissociation barrier. If this isomerization involves migration of atoms or groups, some or all of the energized molecule's degenerate bending modes can then become active hindered internal rotations with an increase in threshold state density and a corresponding increase in the LPL rate constant.[53,54] In C_3H_4 there are certainly many accessible isomers, as is evident from those exhibited in the schematic of Figure 1. Besides the minima shown there, cyclopropylidene[11,55] and various vinylmethylenes, including two low-lying triplets,[12,13] are also well below the fission barrier.

The classical expression for the multiple, two-dimensional hindered-rotor state density given by Kiefer et al.[54] (their eq 10) is

$$\rho_{mHR}(E) = \frac{1}{\sigma(m-1)!}\left[\prod_{i=1}^{m}\frac{2\pi I_i}{h^2}\right]\int_0^{2\pi}\int_{-1}^{1}\cdots\int_0^{2\pi}\int_{-1}^{1}(E - V)^{m-1}H(E-V)\, d\cos\theta_1\, d\phi_1 \ldots d\cos\theta_m\, d\phi_m$$

Here V is the rotor potential and $H(E - V)$ is the Heaviside function which serves to clip any $E < V$. There are many problems in applying this to C_3H_4, but the two most serious lie in the specification of the number of accessible hindered rotors and their hindering potentials. These require far more knowledge of this multidimensional surface than is presently available, so we shall apply the much simpler Whitten−Rabinovitch[56,57] (WR) type estimate discussed at length in ref 54. It is most

convenient to use their final expression for the state density increase over the harmonic density, which is expressed there as an $F_{\text{int-rot}}$, their eq 31, which includes a convolution with the remaining oscillators:

$$F_{\text{int-rot}} = \frac{f_c Q_{m\text{FR}} \prod_j^m (h\nu_j)^2}{(kT)^m} \left[\frac{(s-1)![E + (aE_z)_r - V_b]^{s-m-1}}{(s-m-1)![E + (aE_z)_s]^{s-1}} \right]$$

Here s is the total number of internal modes with m 2-D rotors, leaving $s - 2m$ oscillators. The f_c is a factor which corrects for interaction between rotors, Q_m is the classical free-rotor partition function for the $2m$ rotors, and V_b is a constant or average hindering potential. The rest is standard WR form, and Kiefer et al. recommended the factor a, which corrects for the overcount of states in the Marcus−Rice approximation, be taken from the usual formulas[58] with

$$\beta = \left(\frac{s-1}{s}\right)\left(\frac{s+m}{s}\right)\frac{\langle \nu^2 \rangle}{\langle \nu \rangle^2} \qquad w(E) \rightarrow w(E - V_b)$$

The above result is a simple extension of the WR formulas to the case of m hindered 2-D rotors moving in a constant hindering potential. When such a constant potential is appropriate for the rotors, it should be quite accurate in RRKM calculations, where it will be used only for the molecular density at high energies. This works well on HCN and acetylene,[53,54] using an average potential for V_b in the first instance and the vinylidene energy in the latter. As is evident from Figure 1, the potential for configurational isomerization is, however, by no means constant here. Our problem thus devolves to a specification of the number of rotors, m, and some kind of average V_b.

An identification of the lowest-energy routes for isomerization, routes which lead to hindered rotation in C_3H_4, is illustrated here. The first two rotors are independent rotations of CH_3 and H:

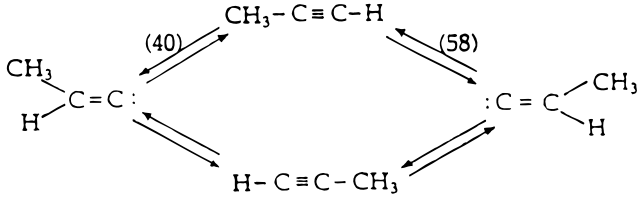

Another H-atom provides a third rotor:

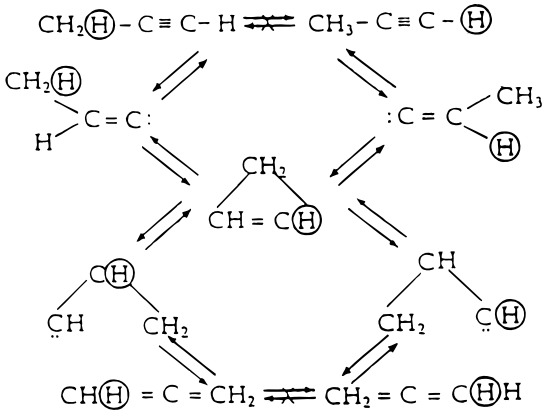

Here the first two rotors are fairly obvious, involving rotation of the acetylenic H-atom in propyne to propenylidene, and rotation of the methyl group to the same result. Fortunately, the barrier for direct methyl rotation in propyne has been calculated by Yoshimine et al.[13] as 61.3 kcal/mol, and it may be 1−2 kcal lower, as before. Note that rotation of the methyl can also be accomplished through cyclopropene via TS4 and TS3 of Figure 1 with a nearly identical barrier of 60.8 kcal/mol (59.5). The third rotor in the above scheme is much less obvious. This is taken to be a second H-atom, one of the methyl hydrogens in propyne, whose motion accesses allene and cyclopropylidene, cyclopropene, and the vinylmethylenes. Again there is more than one path for this rotation, and two possibilities are shown. One can also initiate rotation of an H-atom or a methyl from allene through cyclopropylidene,[13] but this has a higher barrier, above 70 kcal/mol. The direct 1,3-hydrogen shift from allene to propyne evidently has a barrier as high as that for CH fission and can be ignored. Thus this third rotation is not an independent motion like the other two; it can be effected only through complex routes which involve simultaneous motion of the other rotors. To what extent this will restrict its contribution to the threshold state density is unclear, but it would be expected to reduce the accessible phase space through increased rotor interaction. Nonetheless, a third rotor is clearly necessary; without it much of the configuration space, including allene and cyclopropene, would be lost. Also note that there are three degenerate bends available in both allene and propyne.

Having settled on three rotors, it remains to specify the average restriction potential, V_b. Here we have used two potentials, 52 kcal/mol for propyne and 63 kcal/mol for allene. The reason for this is clear from Figure 1: most of the isomers are accessible to lower energies when one starts from propyne. The chosen $V_b = 63$ is just below the barrier to any isomerization from allene, and that for propyne is simply an average of the barriers to H-atom and to methyl rotation, both forming propenylidene. This all seems conservative; certainly the V_b from allene cannot be larger, and from propyne there is also the other more complex route for methyl migration which involves passage through TS3 of Figure 1, whose energy may actually be lower than that for direct methyl rotation.

This model of hindered-rotor effects in the allene/propyne system is little more than qualitative, but any real improvement will be a difficult task indeed. That will require a much greater knowledge of the potential surface for this complex system, including the interaction between rotors which must occur in the several complex isomerization/migration routes that involve simultaneous movement of two or more groups.

The above hindered-rotor model was incorporated into the previous Gorin model RRKM scheme of Table 6 as detailed in Table 7. Here the degenerate bends at 999, 841, and 355 cm^{-1} are considered to convert to internal rotors in allene, and those at 1053, 633, and 328 cm^{-1} are so converted to propyne. One external rotation is again active, and was introduced as prescribed in ref 54. Symmetry numbers, 3 for propyne and 4 for allene, were already assigned through path degeneracies to the external rotations, so there are none for the internal rotors. The moments of inertia for the internal rotors are estimated following the approximate method outlined in ref 54. The f_c is also so estimated. At very high temperatures the introduction of hindered rotation produces some increase in the molecular partition function, and this increase has been calculated and is included in the present RRKM calculations. Below 2000 K the increase is less than 10%, but for propyne at 2222 K it is a factor of 1.4 and becomes 2.3 at 2500 K. The effect is smaller in allene; 1.1 at 2222 K and 1.44 for 2500 K.

The results of calculations with the above $F_{\text{rot-int}}$ inserted into the expression for k_{uni}, using the parameters of Table 7, are

TABLE 7: Hindered Rotor RRKM Model

allene	3015, 1443, 1073, 865, 3007, 1957, 1398, 3086, 3086
propyne	3334, 931, 2918, 2142, 1382, 3008, 3008, 1452, 1452
TS (Gorin)	3310, 3105, 3010, 2107.8, 1445.4, 1044, 964.8, 787.5, 766.85, 548.0, 483.0, 406

Active Moments of Inertia (amu Å^2)

allene	propyne	TS
3.34	3.18	1.7, 53.7, 55.5

I^+/I	$2.15(E_0/kT)^{1/3}$	
E_0 (kcal/mol):	92.5 (from propyne)	91.3 (from allene)
$\langle -\Delta E\rangle_{all}$ (cm^{-1}):	−60 for each	
restriction parameter: $\eta = 1.0 - 2/T$		

6D (3 × 2D) rotor parameters

	allene	propyne
products of moments of inertia (amu Å^2)^3	121.0	121.0
V_b (kcal/mol)	63.0	53.0
f_c	0.72	0.72

compared with the experiments and the earlier "standard" RRKM calculation in Figures 8 and 9. The rates are now up to almost an order of magnitude larger, this arising from a near order-of-magnitude increase in the state density and LPL rate. The new rates are in much better agreement with the experiments in all respects, showing both the desired larger rates and a much greater falloff from second order. The slightly larger rates and notably greater falloff seen in propyne are also both in accord with the present results. Here these are a consequence of the enhanced LPL rate in propyne, relative to allene, which arises from the higher hindered-rotor state density deriving from its lower V_b of 53 kcal/mol. This reduced hindering potential thus offers a reasonable and successful explanation for the greater rate observed in propyne.

Summary and Conclusions

The laser-schlieren data presented here show the process is a very weak chain reaction, almost certainly initiated by C−H fission of the C_3H_4. Other possible dissociation channels were considered at length, including the presentation of new ab initio barriers for the two lowest-energy H_2 eliminations: cyclopropene to cyclopropadienyl, and allene to propadienylidene. The former has much too large a barrier, and the latter suffers from a low entropy of activation but may still make some small contribution. The chain is weak, showing only a faint acceleration, because the parent C_3H_4 act as efficient inhibitors, consuming H-atom chain carriers by abstraction and leaving only the relatively stable propargyl to continue the chain.

A mechanism has been constructed, largely on literature rates, which models both the LS gradients and the TOF product profiles extremely well. Nonetheless, the mechanism is at best schematic; the formation of aromatics and extensive polymerization which occurs in this pyrolysis, leading ultimately to soot, implies a very complex process late in the reaction, which the assumed mechanism cannot hope to describe. This mechanism should be regarded as essentially a short-time description, more than adequate for the few microseconds observed in the LS experiments and thus for extrapolation to the time origin in these, and for the longer but still brief observation of major products in the TOF experiments. The important but difficult issue of the path to benzene and other aromatics is off the main track of this paper and is treated here only in the simplest way, including only the propagyl dimerization path without an adequate

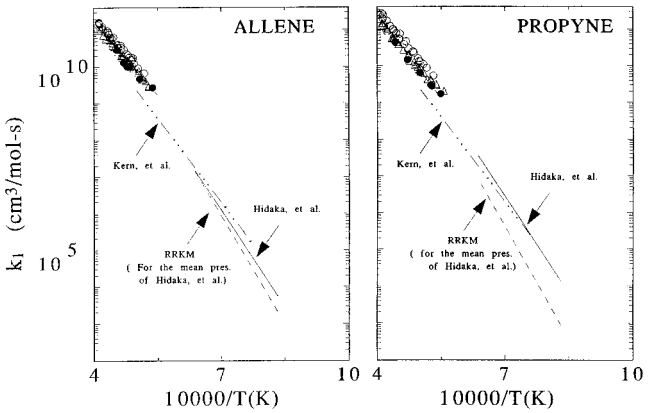

Figure 13. Comparison of literature rate constants for the C−H fission in allene and propyne. The current data are presented in Figure 8 and 9. Literature rates are identified on the figure. Also shown is an estimate of the rate for the 1.7−2.6 atm pressures of ref 10 using the RRKM model of Table 7.

treatment of the complexities of even this reaction.[6] This is probably the major route under most conditions,[3,5] but there are other possibilities.[1]

The principal result here is the set of rate constants for C−H fission of the C_3H_4 isomers displayed in Figures 8 and 9. These were obtained by the extrapolation cum iteration procedure outlined above, which uses the full pyrolysis mechanism to estimate the gradient at $t = 0$. Here only the parent is present, and the vibrationally relaxed state of the gas is unambiguous. Then the only issue in the extraction of a dissociation rate is the ΔH of the reaction, here derived from the 92.5 kcal/mol propyne bond energy computed by Bauschlicher and Langhoff.[31] The derived rate constants are nearly proportional to this heat of reaction, so they are rather insensitive to its exact value. The only significant issues in these rate constants, besides the usual random errors, concern the possible contribution of other channels, discussed above, and the question of whether isomerization is sufficiently rapid to mix the allene and propyne so that separate rates cannot be obtained from the two isomers. Unfortunately their rate of mutual isomerization under low-pressure, high-temperature conditions is in some doubt, but it is unlikely to be so fast that separate rates cannot be resolved. Slightly different rates are actually obtained, a larger magnitude with less deviation from the LPL in propyne, which supports this contention.

The CH fission rate constants of Figures 8 and 9 are compared with the limited literature data in Figure 13. In general the present rates are higher, though not far from the results of Hidaka et al.[10] This is not surprising inasmuch as the literature rates are mainly at lower temperatures and higher pressures and should show a greater falloff. The figure also shows an attempt to predict the Hidaka data using the RRKM model of Table 7, but this then has too much falloff, especially in propyne. This could be from problems with the measurements, which are rather indirect, or it could indicate a poor HPL rate in the model.

The LS second-order rate constants in both isomers are large, and rates obtained from a standard Gorin model RRKM calculation are much too small and have too little falloff from the LPL. Both features are clearly a result of an unusually large LPL rate in these molecules, which cannot be matched in the calculations without introducing an unacceptably large collision efficiency and/or rate of energy transfer. The problem can be resolved by recognizing the wide range of isomers accessible to energies well below the fission barrier in these molecules. In the activated molecule this isomerization converts degenerate bending modes to hindered rotors with a concommitant increase

in threshold state density and LPL rate. The simplified Whitten−Rabinovitsch expression given by Kiefer et al.[54] for the hindered-rotor state density, assuming three rotors with reasonable estimates for the restricting barriers, produces an increase of the required magnitude in the LPL rate. Through a lower barrier to rotation in propyne, it also explains the larger rates and lower falloff observed in this isomer.

The increase in rate seen here from the involvement of hindered rotors is more than twice that found in HCN and C_2H_2. Recognizing that there are more vibrations to share the energy in allene/propyne and the dissociation energy is also much closer to the isomerization barriers, this is rather surprising. There are several reasons for the large effect seen here. The first is simply the number of rotors; with six total rotors one begins to see a big combinatorial effect. Also, with a dissociation barrier not that much larger than V_b, the size of the hindered rotor effect is extremely sensitive to the energy of the activated molecule. Here, because this dissociation now occurs well away from the LPL, reaction actually takes place from considerably above threshold. For example, in propyne at 2000 K and 607 Torr, the maximum contribution to the above RRKM integral for the unimolecular rate is from energies 26 kcal/mol above threshold. For 2000 K and 155 Torr, this is still at 23.5 kcal/mol over threshold. The result is a great increase in the hindered-rotor effect. It is worth observing that the equations actually give almost no increase in the true LPL rate, the rate exactly at threshold. The rate enhancement seen here is thus a falloff phenomenon; the hindered rotors just push the reaction farther from the LPL.

The notion of hindered-rotor enhancement of the state density offers a reasonable rationale for the large rates and low falloff in allene and propyne dissociation. The application of this concept to these large and complex molecules with their extensive isomerization is here crude at best but cannot be easily improved without much more detailed knowledge of the C_3H_4 surface. Even then the problem will be complicated by interaction between the rotors, which are not all independent. Nonetheless, the success of the simple theory applied herein certainly suggests that it carries the right physics to account for the remarkably rapid dissociation seen in these molecules.

Appendix

All calculations were performed with the GAUSSIAN 94[60] implementation of density functional theory (DFT) with 6-311+G-(2d,2p) and 6-311++G(3df,3pd) basis sets.[61] The optimizations were performed using the Flatcher−Powell method and the default GAUSSIAN convergence criteria. A standard search for transition-state structures was performed with HF[62] methods and HF/6-31G* optimized structures was used for further DFT study. A hybrid B3LYP method employing Becke's three-parameter functional[63] has the form $AE_x^{\text{Slater}} + (1 - A)E_x^{\text{HF}} + B\Delta Ex^{\text{Becke}} + Ec^{\text{VWN}} + C\Delta E_c^{\text{nonlocal}}$; the nonlocal correlation is provided by the LYP[64] expression and was used for our final computational studies. The constants A, B, and C are those determined by Becke from fitting the G1 molecular basis set.

Frequency calculations were performed for all structures at the B3LYP/6-311+G(2d,2p) theory level in order to determine the nature of the stationary points. The harmonic approximation for the zero-point energies was used to calculate vibrational adiabatic reaction barriers. All transition-state structures have one and only one imaginary frequency with motion along the reaction coordinate. Energies were also evaluated with B3LYP/6-311++G(3df,3pd) theory level on B3LYP/6-311+G(2d,2p) geometries, and zero-point corrections obtained with B3LYP/6-311+G(2d,2p) theory level were then used.

Acknowledgment. The authors gratefully acknowledge the invaluable assistance to S. S. Kumaran with the RRKM calculations reported herein. This research was supported by the U.S. Department of Energy, Office of Basic Energy Sciences, under Grants DE-FG02-85ER13384 (J.H.K.), DE-FG05-85ER13400 (R.D.K.), and NERSC-ERDP 8854 (B.J. and R.D.K.).

References and Notes

(1) Wu, C. H.; Kern, R. D. *J. Phys. Chem.* **1987**, *91*, 6291.
(2) Alkemade, V.; Homann, K. H. *Z. Phys. Chem.* **1989**, *19*, 161.
(3) Stein, S. E.; Walker, J. A.; Suryan, M. M.; Fahr, A. *Twenty-Third Symposium (Int'l.) on Combustion*; The Combustion Institute; Pittsburgh, 1990; p 85.
(4) Communal, F.; Thomas, S. D.; Westmoreland, P. R. *Twenty-Third Symposium (Int'l.) on Combustion*; The Combustion Institute; Pittsburgh, 1990; Poster P40.
(5) Miller, J. A.; Melius, C. F. *Combust. Flame* **1992**, *91*, 21.
(6) Melius, C. F.; Miller, J. A.; Evleth, E. M. *Twenty-Fourth Symp. (Int.'l) on Combustion*; The Combustion Institute: Pittsburgh, 1993; p 621.
(7) Levush, S. S.; Abadzhev, S. S.; Shevcchuk, V. U. *Neftechimia* **1969**, *9*, 215.
(8) Lifshitz, A.; Frenklach, M.; Burcat, A. *J. Phys. Chem.* **1976**, *80*, 2437.
(9) Hidaka, Y.; Chimori, T.; Suga, M. *Chem. Phys. Lett.* **1985**, *119*, 435.
(10) Hidaka, Y.; Nakamura, T.; Miyauchi, A.; Shiraishi, T.; Kawano, H. *Int. J. Chem. Kinet.* **1989**, *21*, 643.
(11) Honjou, N.; Pacansky, J.; Yoshimine, M. *J. Am. Chem. Soc.* **1984**, *106*, 5361; **1985**, *107*, 5332.
(12) Yoshimine, M.; Pacansky, J.; Honjou, N. *J. Am. Chem. Soc.* **1989**, *111*, 2785.
(13) Yoshimine, M.; Pacansky, J.; Honjou, N. *J. Am. Chem. Soc.* **1989**, *111*, 4198.
(14) Walsh, R. J. *J. Chem. Soc., Faraday Trans. 1* **1976**, *72*, 2137.
(15) Karni, M.; Oref, I.; Barzilai-Gilboa, S.; Lifshitz, A. *J. Phys. Chem.* **1988**, *92*, 6924.
(16) Kakumoto, T.; Usirogouchi, T.; Saito, K.; Imamura, A. *J. Phys. Chem.* **1987**, *91*, 183.
(17) Lifshitz, A.; Frenklach, M.; Burcat, A. *J. Phys. Chem.* **1975**, *79*, 1148.
(18) Bailey, I. M.; Walsh, R. J. *J. Chem. Soc., Faraday Trans. 1* **1978**, *74*, 1146.
(19) Kiefer, J. H.; Kumaran, S. S.; Mudipalli, P. S. *Chem. Phys. Lett.* **1994**, *51*, 224.
(20) Pamidimukkala, K. M.; Kern, R. D.; Patel, M. R.; Wei, H. C.; Kiefer, J. H. *J. Phys. Chem.* **1987**, *91*, 2148.
(21) Pedley, J. B.; Naylor, R. D.; Kirby, S. P. *Thermochemial Data of Organic Compounds*, 2nd ed.; Chapman and Hall: London, 1986.
(22) (a) Kiefer, J. H. In *Shock Waves in Chemistry*; Lifshitz, A., Ed.; Marcel Dekker: New York, 1981; p 219. (b) Kiefer, J. H.; Manson, A. C. *Rev. Sci. Insttrum.* **1981**, *52*, 1392.
(23) Kern, R. D.; Xie, K. *Prog. Energy Combust. Sci.* **1991**, *17*, 191.
(24) Gardiner, W. C.; Hidaka, Y.; Tanzawa, T. *Combust. Flame* **1981**, *40*, 213.
(25) Shimanouchi, T. *Table of Molecular Vibrational Frequencies, I*; NSRDS-NBS, No. 39, US GPO, Washington, 1972.
(26) Tanzawa, T.; Gardiner, W. C., Jr. *J. Phys. Chem.* **1980**, *84*, 236.
(27) Kiefer, J. H.; Mizerka, L. J.; Patel, M. R.; Wei, H.-C. *J. Phys. Chem.* **1985**, *89*, 2013.
(28) Kiefer, J. H.; Shah, J. *J. Phys. Chem.* **1987**, *91*, 3024.
(29) Kiefer, J. H.; Kumaran, S. S.; Sundaram, S. *J. Chem. Phys.* **1993**, *99*, 3531.
(30) Bessaris, G. J.; Kiefer, J. H.; Zhang, Q.; Walker, J. A.; Tsang, W. *Int. J. Chem. Kinetic.* **1995**, *27*, 691.
(31) Bauschlicher, C. W.; Langhoff, S. R. *Chem. Phys. Lett.* **1992**, *193*, 380.
(32) *JANAF Thermochemical Tables*; Natl. Stand. Ref. Data Ser., U.S., Natl. Bur. Stand., Washington, 1985; No. 14.
(33) Kiefer, J. H.; Sidhu, S. S.; Kern, R. D.; Xie, K.; Chen, H.; Harding, L. B. *Combust. Sci. Technol.* **1992**, *82*, 101.
(34) Clauberg, H.; Minsek, D. W.; Chen, P. *J. Am. Chem. Soc.* **1992**, *114*, 99.
(35) Jonas, V.; Bohme, M.; Frenking, G. *J. Phys. Chem.* **1992**, *96*, 1640.
(36) Burcat, A. *Combustion Chemistry*; Gardiner, W. C., Jr., Ed.; Springer: Berlin, 1984; p 455.
(37) Honjou, H.; Yoshimine, M.; Pacansky, J. *J. Phys. Chem.* **1987**, *91*, 4455.
(38) (a) DeFrees, D. J.; McLean, A. D. *Astrophys. J.* **1986**, *308*, L31. (b) Defrees, D. J.; McIver, R. T., Jr.; Hehre, W. J. *J. Am. Chem. Soc.* **1980**, *102*, 3334.

(39) Mollaaghababa, R.; Gottlieb, C. A.; Vrtilek, J. M.; Thaddeus, P. *J. Chem. Phys.* **1993**, *99*, 890.

(40) Kollmar, H. *J. Am. Chem. Soc.* **1978**, *100*, 2660. Tsang, H.-T.; Li, W.-K. *J. Mol. Struct.* **1983**, *104*, 95.

(41) Thomas, S. D.; Communal, F.; Westmoreland, P. R. *Prepr. Pap.-Am. Chem. Soc. Div. Fuel Chem.* **1991**, *36*, 1448.

(42) Kern, R. D.; Chen, H.; Qin, Z.; Xie, K. *Ninteenth Symp. (Int.) on Shock Waves*; Springer: New York, 1993; p 113.

(43) Kern, R. D.; Chen, H.; Kiefer, J. H.; Mudipalli, P. S. *Combust. Flame* **1995**, *100*, 177.

(44) Huntsman, W. D.; Wristers, H. J. *J. Am. Chem. Soc.* **1963**, *85*, 3308; **1967**, *89*, 342.

(45) Pfefferle, L. D.; Boyle, J.; Bermudez, G. *Preprints of Div. of Fuel Chemistry*; American Chemical Society: Washington, 1991, 36: 4,1443.

(46) Kiefer, J. H.; Mitchell, K. I.; Kern, R. D.; Yong, J. N. *J. Phys. Chem.* **1988**, *92*, 677.

(47) Benson, S. W.; Golden, D. M. In *Physical Chemistry. An Advanced Treatise*; Eyring, H., Hendersoll, D., Jost, W., Eds.; Academic Press: New York, 1975; Vol. 7.

(48) Smith, G. P.; Golden, D. M. *Int. J. Chem. Kinet.* **1978**, *10*, 489.

(49) Troe, J. *Ber. Bunsen-Ges. Phys. Chem.* **1983**, *87*, 161.

(50) Troe, J. *J. Chem. Phys.* **1977**, *66*, 4758.

(51) (a) Tsang, W. *Combust. Flame* **1989**, *78*, 71. (b) Tsang, W.; Hampson, R. F. *J. Phys. Chem. Ref. Data* **1986**, *15*, *No. 3*, 1087.

(52) Tsang, W.; Kiefer, J. H. In *The Chemical Dynamics and Kinetics of Small Radicals, Part I*; Liu, K., Wagner, A., Eds.; World Scientific: Singapore, 1995; p 58.

(53) Wagner, A. F.; Kiefer, J. H.; Kumaran, S. S. *24th Symposium (Int'l) on Combustion*; The Combustion Institute, Pittsburgh, 1992; p 613.

(54) Kiefer, J. H.; Mudipalli, P. S.; Wagner, A. F.; Harding, L. B. *J. Chem. Phys.* **1996**, *105*, 8075.

(55) Valtaganos, P.; Elbert, S. T.; Xantheas, S.; Ruedenberg, K. *Theor. Chim. Acta* **1991**, *78*, 287.

(56) Whitten, G. Z.; Rabinovitch, B. S. *J. Chem. Phys.* **1963**, *38*, 2466.

(57) Whitten, G. Z.; Rabinovitch, B. S. *J. Chem. Phys.* **1964**, *41*, 1833.

(58) Robinson, P. J.; Holbrook, K. A. In *Unimolecular Reactions*; Wiley: New York, 1972.

(59) Gilbert, R. G.; Luther, K.; Troe, J. *Ber. Bunsen-Ges. Phys. Chem.* **1983**, *87*, 169.

(60) Frisch, M.; Trucks, G. W.; Schlegel, H. B.; Gill, P. M. W.; Johnson, B. G.; Robb, M. A.; Cheeseman, J. R.; Keith, T.; Peterson, G. A.; Montgomery, J. A.; Raghavachari, K.; Al-Laham, M. A.; Zakrzewski, V. G.; Ortiz, J. V.; Foresman, J. B.; Peng, C. Y.; Ayala, P. Y.; Chen, W.; Wong, M. W.; Andres, J. L.; Replogle, E. S.; Gomperts, R.; Martin, R. L.; Fox, D. J.; Binkley, J. S.; Defrees, D. J.; Baker, J.; Stewart, J. P.; Head-Gordon, M.; Gonzalez, C.; Pople, J. A. *Gaussian 94*; Revision B.3; Gaussian, Inc.: Pittsburgh, PA, 1995.

(61) Frisch, M. J.; Frisch, A.; Foresman, J. B. *Gaussian 94 User's Reference*; Gaussian, Inc.: Pittsburgh, PA, 1995.

(62) (a) Roothan, C. C. J. *Rev. Mod. Phys.* **1951**, *23*, 69. (b) Pople, J. A.; Nesbet, R. K. *J. Chem. Phys.* **1959**, *22*, 571. (c) McWeeny, R.; Dierksen, G. *J. Chem. Phys.* **1968**, *49*, 4852.

(63) Becke, A. D. *Phys. Rev. A* **1988**, *38*, 3098.

(64) (a) Lee, C.; Yang, W.; Parr, R. G. *Phys. Rev. B* **1988**, *37*, 785. (b) Mielich, B.; Savin, A.; Stoll, H.; Preuss, H. *Chem. Phys. Lett.* **1989**, *157*, 200.

(65) Kiefer, J. H.; Budach, K. A. *Int. J. Chem. Kinet.* **1984**, *16*, 679.

(66) Warnatz, J. *Combustion Chemistry*; Gardiner, W. C., Jr., Ed.; Springer: Berlin, 1984; p 197.

(67) Hsu, D. S. Y.; Lin, C. Y.; Lin, M. C. *Twentieth Symposium (Int'l) on Combustion*; The Combustion Institute: Pittsburgh, 1985; p 379.

(68) Frank, P.; Braun-Unkhoff, M. *Proc. 16th Int. Symp. on Shock Tubes and Waves*; VCH: Aachen, 1987; p 379.